

Ramazan Selver

Experiments on the Transition from the Steady to the Oscillatory Marangoni Convection of a Floating-Zone under Various Cold Wall Temperatures and Various Ambient Air Temperature Effects

The transition from the steady to the oscillatory Marangoni convection of a floating-zone under various cold wall temperatures and various ambient air temperature effects have been investigated experimentally by heating the sample from above (opposite direction of Marangoni convection and buoyant forces). The heat transfer takes place mainly through conduction as well as the natural convection of the air around the cylindrical liquid bridge. The ambient airflow in the present work is varied by varying the cold wall temperature and ambient air temperature. In this study, the transition from the steady to the oscillatory Marangoni convection flow of a high Prandtl number fluid in a floating half-zone is visualized by means of the already proven method of the "light-cut-technique". The test fluid zone is held in ambient air at +4 °C, +10 °C, +16 °C, +23 °C, and +28 °C. The onset of oscillations, the oscillation level, and oscillation pattern are investigated under various conditions. It is found that the critical temperature difference (ΔT_c) varies substantially when the cold wall temperature and the ambient air temperature are varied.

1. Introduction

Heat and mass transfer in the crystal growth process are considered to be important in determining the quality of the crystal. Recently, much attention has been given to the effect of thermocapillary flow in crystal growth. Experimental, theoretical, and numerical efforts have been performed to understand thermocapillary convection and essential transport phenomena processes driven by a temperature gradient. The most significant of these transport phenomena is the flow induced, due to the variation in surface tension. The buoyancy generated transport phenomena is considered to be detrimental for material processes (e.g. crystal growth) and its outer space offers a microgravity environment where this transport phenomena is greatly suppressed. In the absence of gravity, the surface tension induced flows become dominant and affect the whole of the fluid and therefore can neither be neglected nor ignored.

Surface tension exists on the interface of two different fluids as the molecules at the interface have higher potential energy than other bulk molecules. This surface tension is not constant and is a function of temperature concentration or electric potential depending upon the nature of the fluid. The surface tension value decreases monotonically with increasing temperature for most liquids. This means that once a temperature gradient exists on the interface that the surface tension also varies along the interface.

The surface tension variation, due to the temperature gradient, induced a tangential stress at the interface which in turn can only be balanced by the shear stress inside the liquid. The stress balance results in the fluid motion at the interface which is transmitted inside the bulk due to the viscosity. These flows, where motion arises due to the variation of the surface tension with temperature, are called thermocapillary flows and are the focus of this present work.

Thermocapillary flows are present in so many practical appli-

Author:

Ramazan Selver
Suleyman Demirel University, Engineering Faculty, Mechanical Engineering
Department, 32260, Isparta, Turkey; e-mail: rselver@mmf.sdu.edu.tr
Phone: (90) 246 211 12 45, Fax: (90) 246 237 08 59

Paper submitted:
Submission of final revised Version:
Paper finally accepted:

cations such as; containerless processing of materials, pools of molten metal formed in welding, spread of flames over liquid fuels, certain processes for growth of crystals and certain two-phase flows like nucleate boiling etc. In a microgravity environment, the influence of thermocapillary flows becomes stronger to the point that in certain circumstances it dominates the other transport mechanisms [1].

The study of combined thermocapillary and buoyancy driven convection flows in a half-zone configuration is divided into two parts, i.e. the study of steady flows and the study of the characterization of oscillatory flows. The study on steady flows is limited to scaling and theoretical analysis as the experimental studies on steady flows in the half-zone thermocapillary configuration done by Kamotani et al. [2, 3] and Chun et al. [4] are considered adequate for temperature oscillations on thermal Marangoni convection in a floating-zone.

The majority of both experimental and theoretical studies on Bénard-Marangoni convection deal with fluids with high Prandtl number from the viewpoint of pattern formation in dissipative systems by Eckert et al. [5]. Typically, such flows have small Reynolds number and are either stationary or are only weakly time-dependent. Surface-tension-driven Bénard convection in low-Prandtl number fluids (zero-Prandtl number limit and a finite Prandtl number corresponding to liquid sodium) is studied by means of direct numerical simulation (Boeck et al. [6]). Boeck and Thess [6] computed in a three-dimensional rectangular domain with periodic boundary conditions in both horizontal directions and either a free-slip or no-slip bottom wall using a pseudospectral Fourier-Chebyshev discretization.

The transition from the steady to the oscillatory Marangoni convection in a floating zone under reduced gravitational influence is visualized by means of the already proven method of the “lightcut- technique” by C. -H. Chun et al. [7]. The influence of

buoyant forces due to horizontal temperature gradients in the experiments was studied by Preisser et al. [8]. Experiments of Preisser et al. demonstrated that the oscillatory state of thermocapillary convection has been proved to be a distortion of the laminar state in form of a wave travelling in the azimuthal direction. The numerical analysis is performed only for steady flows to highlight different aspects of the flow and thermal field. These experiments are performed to determine the onset of oscillations under various conditions. There is a great amount of experimental data available concerning the condition for the onset of oscillations in this condition with high Prandtl number liquids. This data has been obtained by many researchers under various conditions with various experimental procedures. The effects of the buoyancy and the zone interface shapes on the transport phenomenon for the onset of oscillations are carefully assessed under various conditions, as discussed by Masud et al. [3]. In the linear stability analysis, the effect of heat loss on the onset of oscillations has been investigated by Kuhlmann et al. [9] which showed that the heat loss must be appreciable for it to have an important effect for high Prandtl number liquid. Not much attention has been given to the effect of heat transfer from the free surface, which was discussed in our past work. The heat transfer effect in more detail from the liquid free surface in the half-zone configuration is investigated in liquid bridges of high Prandtl number fluid. Marangoni convection flow tests are usually placed at room temperature. The heat loss from the liquid free surface is mainly caused by the ambient air motion. The ambient air motion around the liquid is mainly caused by buoyancy due to the nonuniform temperature distribution in the air produced by the heating and cooling done in the tests, as studied by our past work [10]. Due to natural convection of the air, the heat loss can be controlled by adjusting the overall fluid temperature level relative to the ambient temperature [11]. Therefore, the present experiment conditions for the onset of oscillations are investigated under variable natural convection heat transfer. These show that the heat transfer effect is significant.

2. Important Dimensionless Parameters

Silicone oil is used as the test liquid and suspended between two coaxial copper rods which are 3 mm in diameter. The experimental configuration is sketched in Fig. 1. According to Ostrach [12], the important dimensionless parameters for thermocapillary flow in a confined fluid with a flat free surface in the absence of gravity are: the Prandtl number $Pr = \nu/\alpha$, the surface tension Reynolds number $R_\sigma = (\sigma_T \Delta T L) / \mu \nu$, and the zone aspect ratio $Ar = L/D$, where $\Delta T = (T_H - T_C)$ is the maximum temperature difference along the free surface, L is the length of the fluid column, D is the diameter of the test section, ν is the kinematic viscosity, μ is the dynamic viscosity, α is the thermal diffusivity, σ is the surface tension, σ_T is the temperature coefficient of surface tension, and g is the gravitational acceleration. The Marangoni number is defined as $Ma = R_\sigma Pr = (\sigma_T \Delta T L) / \mu \alpha$, and it is an important parameter in thermocapillary flow analy-

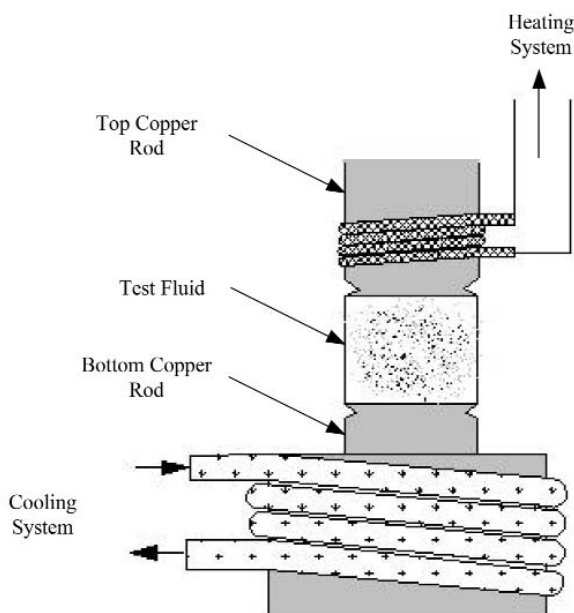


Fig. 1 Test Section.

sis. The liquid column shape can not be made exactly cylindrical due to the effect of gravity. The shape depends mainly on the amount of liquid and the static Bond number $Bo = (\rho g L^2) / (\sigma Pr)$. Small liquid columns are used in order to minimize the effects of buoyancy and gravity, which will be discussed later. It is known that the oscillatory flow structure in the half-zone configuration is sensitive to the free surface shape. Because of some practical constraints in the current experiments, Bo is reduced to unit order or smaller so that the liquid column shape deviates slightly from the cylindrical. The experiment is designed to study convection in a simulated vertically floating halfzone configuration of crystal growth [13].

According to Kamaotani Y. et al. [10], the condition for the onset of oscillations for high Prandtl number (Pr) fluid is specified by two parameters: the Marangoni number (Ma) and a surface deformation parameter [2]. These two parameters must become large enough for the transition to occur. The size of the liquid column is also an important parameter. In the present experiment, the Ma number controls the transition. Therefore, the critical Marangoni number (Ma) is used in the present work.

The ambient air motion around the liquid column is due to natural and forced convection. The natural convection is associated with the temperature differences $(T_H - T_R)$ and $(T_C - T_R)$ and is induced by the overall heating-cooling arrangement of the experiment for a given configuration. The forced convection is due to the thermocapillary convection of the liquid free surface, so the ambient airflow is associated with a temperature difference $(T_H - T_C)$ for a given configuration. Therefore, the overall ambient airflow is sufficiently specified by two temperature differences: $(T_H - T_R)$ and $(T_C - T_R)$ or $(T_H - T_C)$ and $(T_C - T_R)$ [11]. Based on the experimental visualization of the ambient airflow for the present configuration, it has been shown that the liquid free surface heat transfer rate is affected by natural convection. The ambient airflow motion is found to be rather weak at +28 °C (the experimental apparatus and other apparatuses are placed in the room at +28 °C), at the rate of a few cm/s, so it is difficult to investigate it in detail, especially the heat transfer rate on the liquid free surface. However, the airflow motion at cold room temperature, +4 °C (the experimental apparatus and other apparatuses are placed in the room at +4 °C), is found to be much stronger than the airflow motion at room temperature, +28 °C. Based on the experimental study of the airflow for the present configuration, it has been shown that the free surface heat transfer rate is affected by the natural convection which depends on the ambient air temperature. For this reason, the main purpose of the present work is to investigate the direct effect of these temperature differences on the critical condition.

3. Experimental Design

3.1 Experimental Apparatus

The experimental apparatus is set up to simulate the floating-zone configurations for the purpose of studying Marangoni convection, especially the oscillatory phenomenon. The basic com-

ponents of the setup are the fluid, the test section, the temperature measurement system, the heating system, the cooling system, and the flow visualization system. They are given in Fig. 2.

The important considerations in selecting a test fluid for this study are the effect of surface contamination from the environ-

Properties	5 cSt oil	Units
Density (ρ)	913	kg/m ³
Thermal Conductivity (κ)	0.1088568	W/m-K
Thermal Diffusivity (α)	7.42x10 ⁻⁸	m ² /s
Specific Heat (C_p)	1716.588	J/kg-K
Coefficient of Thermal Expansion (β)	0.00105	1/K
Dynamics Viscosity (μ)	4.4554x10 ⁻³	Ns/ m ²
Kinematic Viscosity (ν)	4.88x10 ⁻⁶	m ² /s
Surface Tension (σ)	19.7x10 ⁻³	N/m
Temperature Coefficient of Surface Tension, $-\left \partial\sigma/\partial T\right $	-0.0587x10 ⁻³	N/m-K
Prandtl Number (Pr)	67	

Kinematic viscosity ν (cSt) variation with temperature (°C)

$$\nu = 8.185 - 0.2T + 3.74 \times 10^{-3} T^2 - 4.865 \times 10^{-5} T^3 + 3.474 \times 10^{-7} T^4 - 9.76 \times 10^{-10} T^5 \quad [1]$$

Table 1. Properties of Dow Corning 200 Fluid Silicone Oil at 25 °C [1]

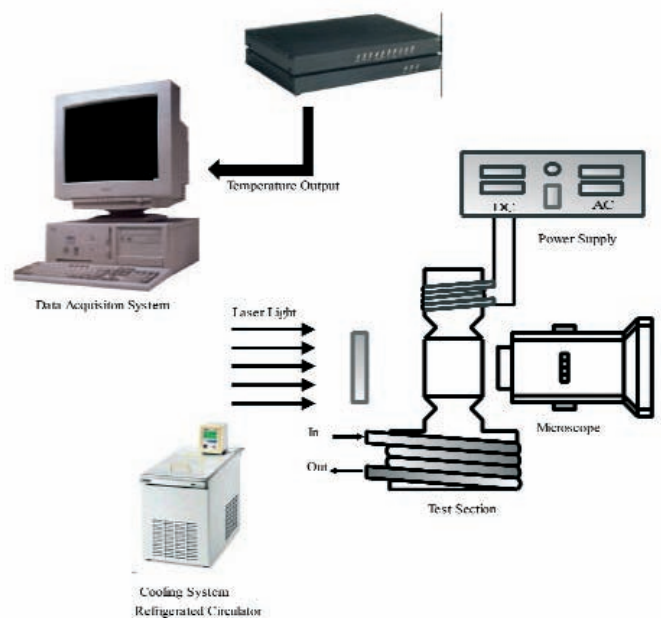


Fig.2 Schematic Diagram of Experimental Setup

ment, zone stability and health hazard involved in the handling of the fluid. The presence of surface active substances may lead to a significant change in the flow. The high surface tension of the fluid in relation to its density enable it to form a stable liquid column. In addition to these requirements, transparency of the test fluid is desired so that the flow visualization can be carried out. The silicone oil that is used is composed of low viscosity Polydimethylsiloxane polymers manufactured by "Dow Corning" to yield essentially linear polymers with an average kinematic viscosity of 5 cSt. Its properties are given in Table 1. Their low viscosity makes it possible to cause a transition to an oscillatory flow at a relatively small temperature difference.

The test section consists of two supporting copper rods, a heating system, and a cooling system. Both rods are machined with our lathe machine. A sharp pinning edge is made in the form of a groove on the rods so that silicone oil could be suspended even if the fluid volume is greater than that of a perfect cylinder. One of the rods is encased in a cooling block to maintain a constant temperature. The cooling block consists of a copper tubing-cooling jacket soldered to a cylindrical copper block in which the rod is embedded with a high thermal conductive paste. The main test frame is common for this experiment and small diameter zones are chosen to generate predominant Marangoni convection. Copper rods which are 3 mm in diameter are used in the experiment. Both have thermocouples embedded. The liquid column length is aligned and varied by controlling the position (x-y-z) traversing screws of the main supporter.

Silicone oil is suspended vertically between two copper rods. The liquid column is slightly noncylindrical due to the small effect of gravity.

Copper-constant thermocouples with a diameter of 0.0508 mm are used for measuring the heating rod temperature and the cooling rod temperature. Copper-constant thermocouples are used in this experiment because of their sensitivity and fast response time. These thermocouples have a high accuracy of 0.05 °C which is sufficient for the present experiment. The choice of the size was made in order to minimize disturbances of the flow near the heater. The thermocouples are connected to an Omega OMB-TEMPSCAN-1100 data acquisition system which has a built-in cold junction compensator. The OMB-TEMPSCAN-1100 is connected to a personal computer in which a ChartView graphic software is installed for controlling and recording data. A sampling rate of 5 times per second is chosen so that the expected frequencies are covered without acquiring excessive data. In the present work, all of the temperature data and the temperature frequency data are taken by thermocouple outputs. The data is stored, processed, and made available for future viewing.

The heating system consists of a DC power supply connected to a heating element. A tin nichrome wire is wound around one of the copper rods to form the heating element as shown in Fig. 2. The heater is connected to a Philip Harris Co. DC power supply of 25 volts and with 10 amp. maximum capacity. The

purpose of the cooling system is to maintain one of the copper rods at a constant temperature.

The cooling system consists of a desired temperature water bath hooked up to the test section with a cooling water circulating mechanism. For this purpose, a Heto HMT 200 digital temperature bath (model CBN 8-30) with distilled water as the cooling medium is used. The bath temperature setting is digitally controllable with a resolution of 0.1 °C.

The flow visualization system is used for observing the flow field and comprises of a microscope. The microscope has a close working distance of around 50 mm. with a 40X magnification. Alumina powder which is 1.5 micron in size is used as the seeding particle for the fluid. A 35 mW He-Ne laser with a cylindrical glass rod to produce a light sheet serves as an illuminating source for the liquid column. By illuminating the alumina particles mixed in the fluid by the laser light sheet, the flow is seen through a microscope and the flow pattern is observed.

3.2 Experimental Procedure

The experiments should be done in a clean environment and isolated from the ambient vibrations because surface tension is so sensitive to contamination. The test section and other apparatuses are set up horizontally on a level table.

The cylindrical copper rods are cleaned with alcohol and dried with clean compressed air. A small amount of barrier coating (Scotch Guard Fabric Protector) is applied to the outer surface of the lower cylindrical rod so that the silicone oil does not spread over the surface and it is allowed to dry completely. This prevents the liquid from running down during the experiments. Both rods are aligned and leveled while being observed through the microscope system at about 40X magnification by using the x-y-z positioned screws.

The length of the column is gradually increased by carefully adding small droplets one at a time using a hypodermic syringe until the desired fluid length (L) and cylindrical shape is obtained. The liquid column length is carefully measured by a dial gauge. It is located at the bottom section of the test equipment.

The DC power supply, temperature measurement device (OMB-TEMPSCAN-1100), the cooling system, and laser beam generator are turned on. After motion has started the flow, the seeding particle is added to the fluid. The particles will sink to the bottom of the fluid if added before the fluid is in motion. The heater power is increased in small steps while observing the flow field. Sufficient time is to be afforded between the increments so that flow field and the heater temperature reach a steady state. This increment in power continues till oscillations are observed through the flow visualization system. The heated rod and cooled rod temperatures are noted at the onset of oscillations. The Marangoni convection is affected by the buoyancy and the liquid column shape by gravity. In our past experiments, we obtained the conclusion that the shape distortion due to gravity is more important than the buoyancy effect and that the error

in the critical temperature difference due to the shape effect can be made within $\pm 6\%$ if the liquid column length is smaller than about 2 mm. For this reason, 3 mm diameter rods are used in the present experiment with the maximum Ar of 0.5 – 1.0. On the other hand, the test section apparatus in certain experiments is covered by a carton box in order to observe the airflow motion around the liquid column free surface. During certain experiments, inert gas (smoke) is slowly injected into the carton box until the airflow motion is observed easily. This inert gas (smoke) does not affect the Marangoni convection flow in the present experiment. During the experiment, air temperature is uniformly maintained. For all experiments with free surface shapes, the liquid volume is adjusted and the procedure is repeated. All tests are repeated at least three times to check repeatability of the data. Then, a comparison is made for the critical temperature differences obtained by these three runs. The average data values are used in all cases.

The ranges of the parameters covered in the present experiment are $Ar = 0.5 - 1.0$, $Pr = 49-60$. For the Ma number and the Pr number, the physical properties of the liquid are evaluated at the average value of the liquid surface temperature, $(T_H + T_C)/2$. The error involved in the measurement of the critical temperature difference (ΔT_{cr}) is estimated to be within 3.5% (average values of at least three experimental data). T_H and T_C are measured with 0.1 °C accuracy. The surrounding air temperature and room temperature are maintained within ± 0.1 °C accuracy.

4. Results and Discussion

In reality, the static free surface of the liquid column has a non-cylindrical shape due to the effect of gravity. The shape is determined by the static Bond number, the fluid volume and the aspect ratio. The fluid shape on test section takes a more cylindrical shape at the smaller static Bond number. The free surface shape is obtained from the balance between the pressure difference across the interface and the surface tension. In the present experiments, for the aspect ratio of 0.5 the shape becomes very close to cylindrical when the fluid volume is made equal to that of a perfect cylinder (relative volume = actual volume / cylindrical volume = 1). The relative volume can not be made equal to unity by increasing the (Ar) because of the large contact angle at the bottom of test fluid. For this reason, the typical ranges of aspect ratio (Ar) have been restricted to a value between 0.5 and 1.0 in the present experiment. It is known from Y. Kamotani et al. [10] that the onset of oscillations was not a strong function of the liquid free surface shape on the oscillatory thermocapillary flow for aspect ratio higher than 1.0.

When the liquid column is gradually heated through the free surface, the gradients of the surface tension induce thermocapillary flow. To minimize buoyancy induced flow, the liquid column is heated from the top rod. A photograph of steady state Marangoni convection is shown in Fig. 3. In this photograph, it is observed that the fluid of the liquid free surface moves from the hot region to the cold region. Two axisymmetric counter-

rotating flow cells in a radial plane are generated due to the mass conservation as shown. The fluid motion extends nearly all the way to the cold wall. As stated previously, the main purpose of this study is to show the effect of heat loss of the liquid free surface. The effects of the ambient air temperatures on the Marangoni convection have been investigated experimentally under normal gravity by heating from above. Therefore, different room temperatures are chosen which are $T_R = + 28$ °C , + 23 °C, + 16 °C, + 10 °C, and relatively low temperature $T_R = + 4$ °C. The results of the analysis for those cases are given in the following paragraphs.

The experiments are conducted with various values of the cold wall temperature (T_C). Room temperature (T_R) is kept constant during these experiments. The fluid zone in the experiment is held in ambient air at + 28 °C , + 23 °C, + 16 °C, + 10 °C, and +4 °C. The cold wall temperature is fixed at a desired value and then the hot wall temperature (T_H) is gradually increased

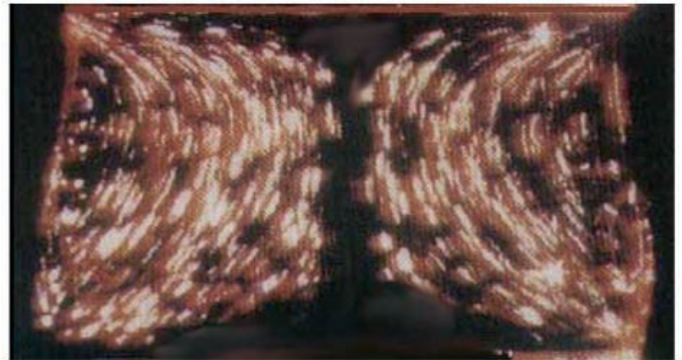


Fig. 3 Photograph of Steady Thermocapillary Flow for $Ar = 0.6$.

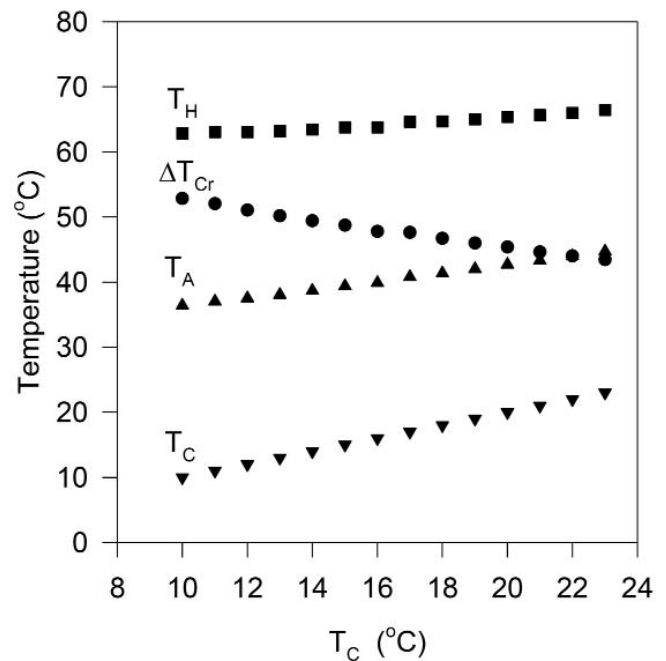


Fig. 4 Effect of T_C on critical condition for $Ar = 0.5$, $D = 3$ mm, $T_R = +28$ (°C).

until the flow structure becomes oscillatory. As the heater temperature is increased, the value of $\Delta T = T_H - T_C$ becomes equal to the critical temperature difference, ΔT_{Cr} , at which point the flow structure becomes oscillatory. It is clear that the flow structure remains basically the same with increasing temperature differences, but beyond a certain temperature difference, the flow structure suddenly changes.

The experimental results of the high and low room temperatures are discussed next. First, experimental results at a fixed room temperature around $+28^\circ\text{C}$ obtained with various values of the aspect ratios and various values of the cold wall temperatures are discussed for the onset of oscillation states. The effect of the cold wall temperature (T_C) on the critical temperature difference (ΔT_{Cr}) in a room at $+28^\circ\text{C}$ is shown in Fig. 4. This figure shows that ΔT_{Cr} decreases with increasing T_C because of decreasing fluid viscosity. The heater temperature (T_H) at the onset of the oscillation condition slightly increases when the (T_C) is increased from 10°C to 23°C . These cold wall temperature variations are sufficient for experimental detection as the following figures show. Therefore, the critical temperature difference is non-dimensionalized as a critical Marangoni number (Ma_{Cr}). The viscosity in the critical Marangoni number was evaluated at the average temperature [$T_A = (T_H + T_C)/2$]. Ma_{Cr} and the critical condition Prandtl number (Pr) of the liquid change with T_C in Fig. 5. The cold wall temperature effect becomes significant in the present experiment.

When the Marangoni number becomes larger than a certain value, oscillatory flow appears. The temperature and velocity fields strongly interact with each other. Consequently, the flow field becomes unstable beyond a certain Marangoni number. The temperature oscillation pattern is measured by a thermocouple in the fluid and observed through a microscope. A fre-

quency between 0.6 and 1.2 Hz. is observed, becoming higher with increasing ΔT . For $Ar = 0.6$ oscillations at a fixed room temperature of $+23^\circ\text{C}$, flow patterns are shown in Fig. 6. The oscillatory flow was not uniform as can be seen in Fig. 7. The phase difference of the temperature oscillation between the two pictures is 180° . If it is compared to the flow pattern in Fig. 3, it is clear that the flow pattern is no longer an axisymmetric flow and it is an oscillatory flow pattern. In Figs. 6,7 the streamlines of the oscillatory Marangoni convection on the zone surface and in a vertical section are sketched for a fixed time. Comparison with experiment shows a good agreement at the aspect ratio $Ar = 0.5-1.0$. The same steady and oscillatory flow patterns are seen in all the tests that have been done in this study. There is a strong resemblance between oscillatory flow pattern of current study and oscillatory flow pattern of Preisser et al.. The moment is depicted when the vortices (rolls) in the light cut have extreme positions. The vortex in one half of the zone section appears smaller than the opposite vortex, and the center of the smaller vortex is located nearer to the lower solid boundary. The larger vortex is characterized by a center closer to the upper copper rod. In the light cut, the time dependence is observed as a periodical interchange of the shape of the vortices in the left and right parts of the zone. After one half of the oscillation period, the left vortex (small) and the right vortex (large) have changed positions. In the total view in Figs. 6,7 the time dependence is shown in the moment of the branching streamline

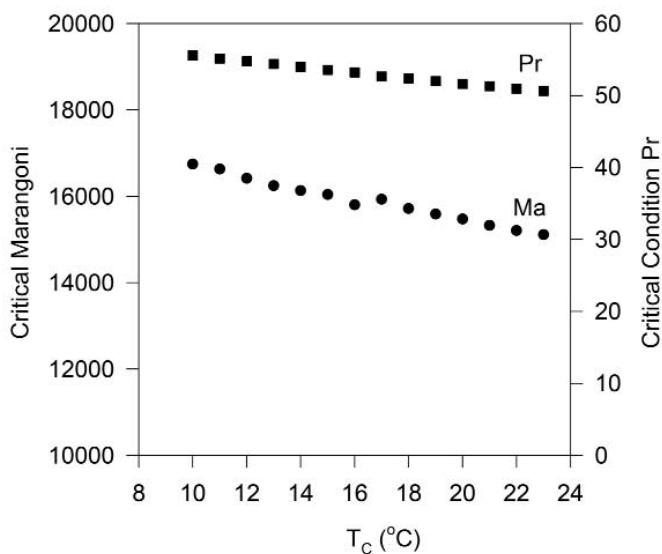


Fig. 5 Effect of T_C on critical condition for $Ar = 0.5$, $D = 3\text{ mm}$, $T_R = +28^\circ\text{C}$.

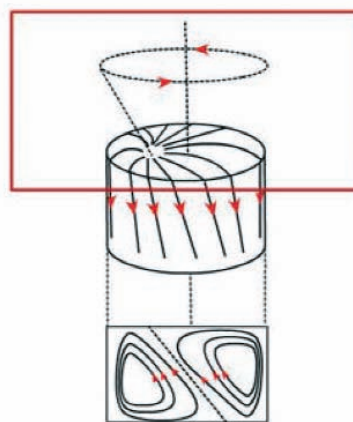


Fig. 6 Photograph of Oscillatory Thermocapillary Flow for $Ar = 0.6$ at $T_R = +23^\circ\text{C}$.

of opposite vortices. The branching streamline rotates with the oscillation frequency around the zone axis in the surface of a cone. While the features of the steady state Marangoni convection roll are independent of the azimuthal angle, the oscillatory state at a fixed time is characterized by a sinusoidal distortion of the roll cross-section and the roll axis azimuthal direction [8]. There is no study the various cold wall temperatures and the various ambient air temperatures effects in the investigation of Preisser et al.. In the present investigation, various cold wall temperatures and various ambient air temperatures effects were carried out for a configuration of an experiment that was focused on the steady and the oscillatory Marangoni convection of a floating-zone. However, Preisser et al. only reported experimental data for molten NaNO_3 on laminar and time-dependent thermocapillary convection in floating zones of various lengths and diameters. NaNO_3 is chemically stable up to approximately 400°C and the melt is fully transparent. Experimental results of Preisser et al. show that the cold wall temperature was almost same as the ambient air temperature. In the present study, the onset of oscillation from the steady to the oscillatory Marangoni convection of a floating-zone under not only various cold wall temperatures but also various ambient air temperatures effects have merely been investigated experimentally by stating steady and oscillatory flow pattern.

The Marangoni convection experiments are conducted at a

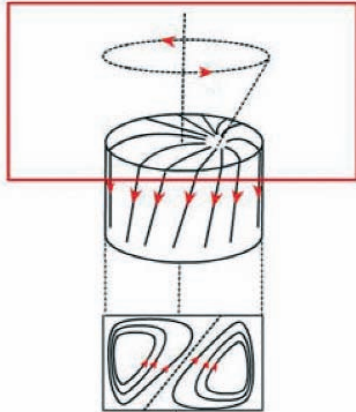


Fig. 7 Photograph of Oscillatory Thermocapillary Flow for $Ar = 0.6$ at $T_R = +23^\circ\text{C}$.

room temperature of $+28^\circ\text{C}$. The heat loss from the liquid free surface is caused by the convective air motion. The radiation heat transfer at the free surface is also important in high temperature level tests. In these experiments, the high temperature tests were not studied. The conditions for the onset of oscillation flows are investigated under various natural convection heat losses in the present experiments. The heat loss rate from the liquid free surface due to natural convection of the air is affected by changing the values of T_C . The natural convection of the air can be controlled by adjusting the overall liquid temperature level relative to the ambient temperature. As seen in Fig. 5, at a fixed room temperature around $+28^\circ\text{C}$ the liquid average temperatures are evaluated for $T_C = +10^\circ\text{C}$ and $T_C = +23^\circ\text{C}$, $T_A = \frac{1}{2}(T_H + T_C)$. These two T_A values are compared with various values of T_C . In the present experiments, T_A for $T_C = +10^\circ\text{C}$ is generally less than T_A for $T_C = +28^\circ\text{C}$, which means that heat is lost from the liquid free surface on the average temperature of the liquid. As a result, the liquid free surface average temperature continuously decreases when decreasing the cold wall temperature (T_C).

The values of the critical temperature difference (ΔT_{Cr}) are shown in Fig. 8 under various cold wall temperatures (T_C) and aspect ratios (Ar). Similar trends were observed under various aspect ratios. Moreover, as the figure shows, the critical temperature difference tends to be higher for small values of the cold wall temperature (T_C). The data is collected from the visualized oscillation seen with the microscope. The overall distributions are almost identical in all cases within the experimental accuracy. As mentioned above, the determination of the onset of

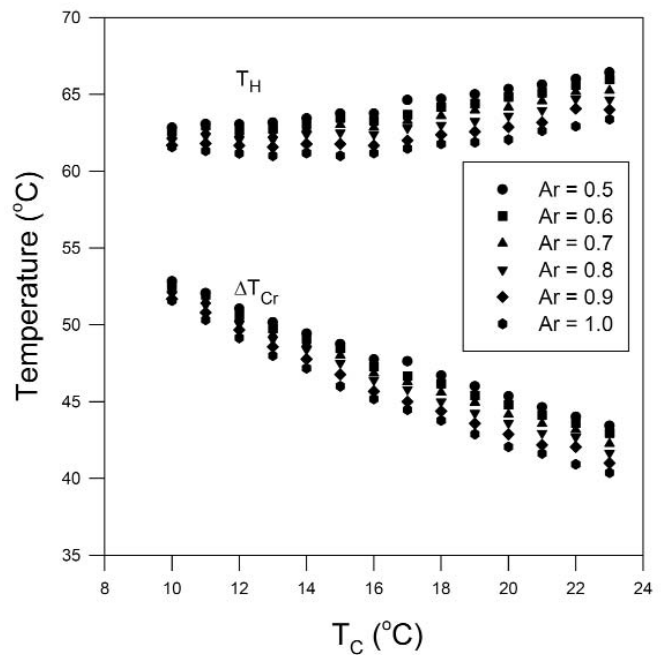


Fig. 8 Critical Temp. Diff. and T_H versus Cold Wall Temp. with Various Aspect Ratios for $T_R = +28^\circ\text{C}$.

oscillations by visual observation is somewhat subjective. However, the same tests are repeated for three times with fresh liquid under the same conditions.

These critical temperature differences are non-dimensionalized as the critical Marangoni number (Ma_{Cr}) based on the height of the liquid column. The values of the Ma_{Cr} are determined under various conditions, i.e. for the various aspect ratios and the various cold wall temperatures. The critical Marangoni number and critical condition Prandtl number versus the cold wall temperature graph are plotted in Fig. 9. The dimensionless

critical conditions are quite consistent among various tests. The critical Marangoni number curves and the critical condition Prandtl number curves in Fig. 9 tend to go down with the increasing cold wall temperature (T_C). The critical Marangoni number (Ma_{Cr}) and the critical condition Prandtl number trends seem to be continuous as seen in the figure. The tendency of the increasing critical Marangoni number (Ma_{Cr}) to increase with the increasing aspect ratio (Ar) is related to the viscous retardation effects of the liquid column height increase with increasing aspect ratio (Ar). Since the onset of oscillations should depend on the Marangoni number for cases having the same aspect ratios, it is expected that the dependence of the critical temperature differences for the onset of oscillations should be inversely proportional to the length. The experimental results verify this relationship. Also, the critical Marangoni numbers decrease with the increasing cold wall temperatures at fixed aspect ratios.

From the above discussion, the results of the cold wall temperature variation at a fixed room temperature of +28 °C were obtained by the extremes of the test sections. The results of the relatively low room temperature $T_R = +4$ °C analysis are discussed. In the typical tests, the temperature of the large experimental room is fixed at +4 °C and then the T_H is gradually increased until the flow structure becomes oscillatory. The cold room temperature (T_R) is constant during the experiment. In the cold room, the critical temperature difference data is useful in understanding the heat loss from the liquid free surface in the thermocapillary flow under these experimental conditions. As explained later, in some of the cases for the cold room ($T_R = +4$ °C) tests, including cases where T_R is smaller than T_C , the liquid column loses heat on the free liquid surface to the surrounding air. The convective air motion along the liquid column is relatively higher for the cold room (+4 °C) tests due to the high temperature differences between the T_A and T_R . Temperatures ver-

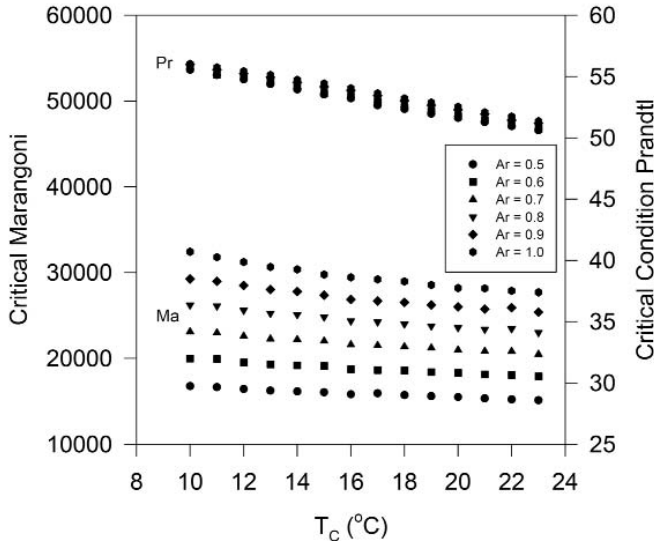


Fig. 9 Critical Ma number and Pr number versus Cold Wall Temp. with Various Aspect Ratios for $T_R = 28$ °C.

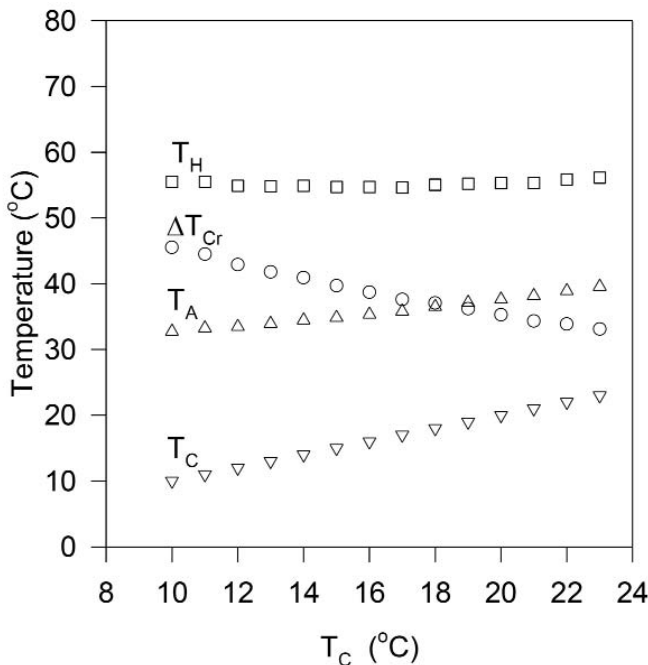


Fig. 10 Effect of T_C on critical condition for $Ar = 0.5, D = 3$ mm, $T_R = +4$ (°C).

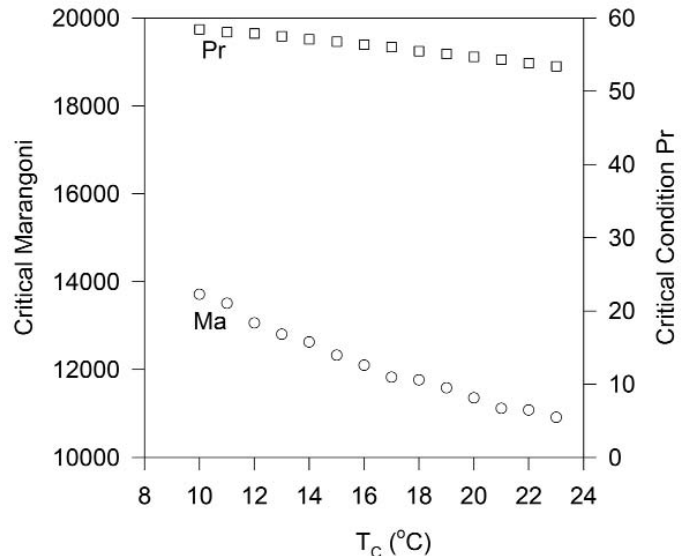


Fig. 11 Effect of T_C on critical condition for $Ar = 0.5, D = 3$ mm, $T_R = +4$ (°C).

sus applied various cold wall temperatures are plotted in Fig. 10 for $Ar=0.5$. This figure shows the critical temperature differences for the liquid column diameter ($D = 3$ mm.) and 5 cSt silicone oil on the same test section under variations in the cold wall temperature conditions. As seen in this figure, the heater temperature at the critical condition remains nearly constant when the cold wall temperature is varied from $+10$ °C to $+23$ °C, which means the critical temperature difference decreases with an increase in the cold wall temperature. It is clearly seen that the values of the critical temperature difference, the heater temperature, and the average liquid temperature in the cold room are much smaller than those in the room temperature ($+28$ °C). Fig. 11 also shows that the Ma_{Cr} value decreases and the critical condition Pr number changes slightly with an increase of the cold wall temperature T_C . Fig. 10 with Fig. 4 are plotted together in Fig. 12 and from Fig. 12, it can be seen that the trends are similar. On careful examination, it can be seen that the critical temperature difference values, the Marangoni number in Fig. 13, and the Prandtl number for the two different ambient air temperature levels have generally similar trends in the present work.

In order to investigate the effect of heat loss on the steady flow in room temperature ($+28$ °C and $+4$ °C) tests, the experimental apparatus is covered with a carton box during a few tests. To take a picture of the convection air motion, a few of the experiments are performed while the apparatus is covered with a carton box. Sufficient inert gas (smoke) was slowly injected into the cardboard box in order to easily observe the convective air motion under the present experimental conditions. The typi-

cal air flow patterns are shown in Fig. 14 which is a photograph taken for $Ar=0.6$. This convective air motion along the liquid column is visible due to the high temperature differences between the T_A and T_R . Therefore, the convective heat transfer from the liquid free surface to the air increases with an increase of the cold wall temperature (T_C).

The observed flow for convective air motion in the cold room is faster than that of room temperature of $+23$ °C but the basic flow structure is similar. If the two convective air motions around the test fluids are compared, the convective air motion at room temperature ($+23$ °C) is smaller, in the present experiment, due mainly to the temperature difference between the ambient air temperature and the average value of the liquid free surface temperature. The convective air motion is a relatively weak natural convection of the surrounding air in the room ($+23$ °C). However, differences are noticeable which signify the influence of the heat loss from the liquid free surface on the flow field. As discussed above, the present heat loss effect is observed only for the liquid bridge with a nearly flat free surface. The temperature oscillation patterns of the thermocapillary flow experiment in the cold room $T_R = +4$ °C are the same as

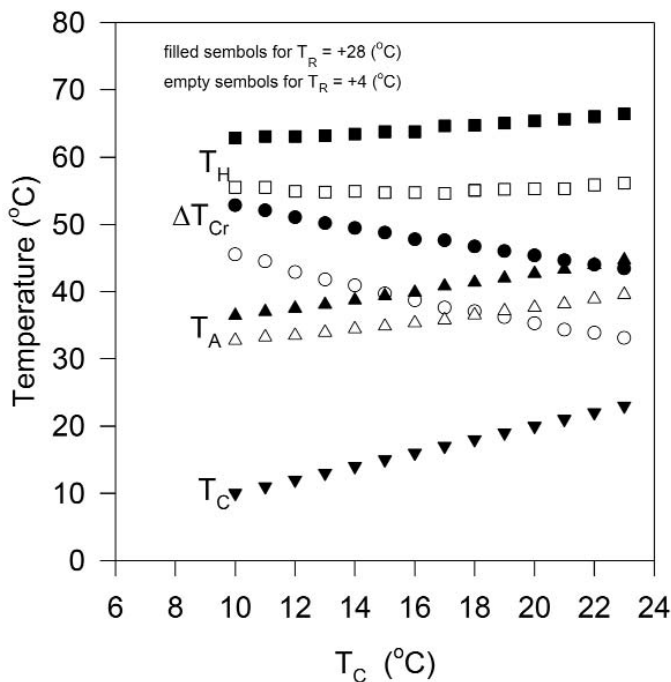


Fig. 12 Comparison data on critical condition between $T_R = +28$ (°C) and $T_R = +4$ (°C) for $Ar = 0.5$.

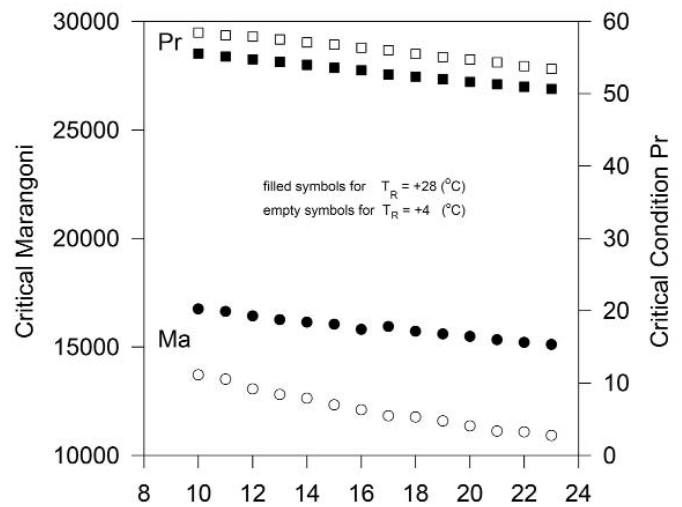


Fig. 13 Comparison data on critical condition between $T_R = +28$ (°C) and $T_R = +4$ (°C) for $Ar = 0.5$.

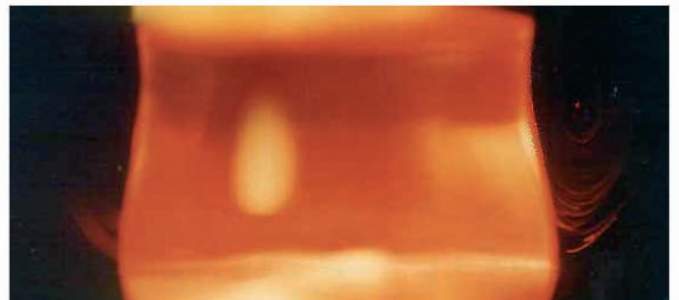


Fig. 14 Photograph of Airflow Motion around Liquid Column (at Cold Room Temp. $+4$ °C, $Ar = 0.6$)

those found in the earlier experiment at room temperature $T_R = +23\text{ }^\circ\text{C}$.

Kamotani et al. [10] suggested that the heat loss from the liquid free surface on the thermocapillary flow field is minimized on the oven test when the highest room temperature T_R is chosen so that it is nearly equal to the average temperature T_A .

Finally, as the values in the present study are shown in Fig.15, it can be seen that the critical temperature difference values in the various room temperatures for $Ar= 0.5$ have noticeable differences. As shown in Fig. 15, the critical temperature difference values at $T_R = +28\text{ }^\circ\text{C}$ are higher because, in the present experiment, the heat loss from the liquid surface becomes small. In other words, the temperature difference between the liquid free surface temperature and the ambient air temperature (room temperature) at a desired cold wall temperature decreases away when increasing the ambient air temperature. Therefore, the results in the relatively lower ambient air temperature are consistent with the results of the relatively higher ambient air temperature due to the heat loss from the liquid free surface.

The critical temperature difference (ΔT_{Cr}) curves in Fig. 15 tend to go down with the decreasing ambient air temperature (room temperature T_R). The trend of the critical temperature difference seems to be continuous as seen in the figure. The tendency of the critical temperature difference (ΔT_{Cr}) to decrease with ambient air temperature T_R is related to the fact that the heat loss effects of the liquid free surface increase with the decreasing ambient air temperature (room temperature T_R).

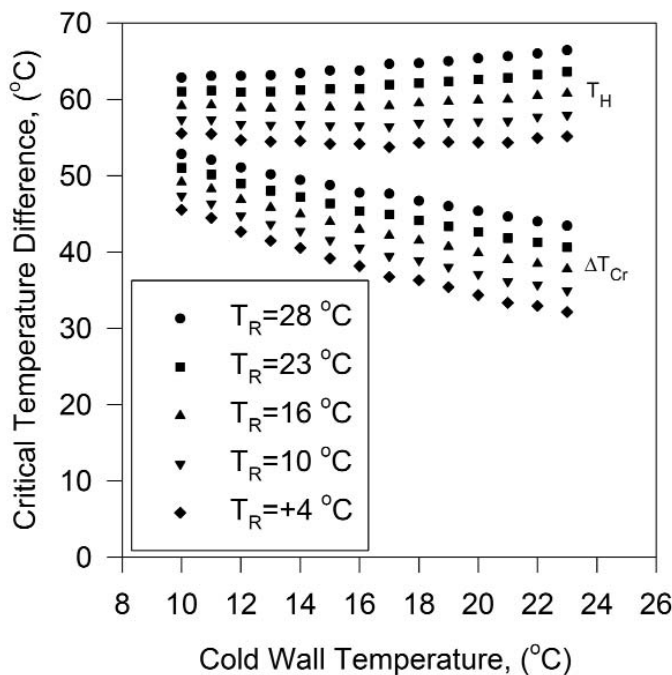


Fig. 15 Critical Temp. Diff. and T_H versus Cold Wall Temp. with Various Room Temperature for $Ar=0.5$, $D=3\text{ mm}$.

The onset of oscillations depend on the critical temperature difference as was explained in this study. As a result, it is expected that the dependence of the critical temperature differences for the onset of oscillations should be proportional to the convection heat loss from the liquid free surface to the ambient air.

5. Conclusions

The present study focuses on the effect of cold wall temperature variations and the effect of liquid free surface heat loss on the onset of oscillatory thermocapillary flow with a high Prandtl number fluid. The different ambient air temperatures have been studied for this purpose. The critical temperature difference varies when the cold wall temperature and the ambient air temperature are varied. The heat loss at the liquid free surface is identified to be responsible for this effect. This shows that the critical temperature differences decrease with an increasing heat loss. The present study shows that the condition of the surrounding convective air motion has to be known for comparing various data on the onset of the temperature oscillations on the thermocapillary flow in a floating half-zone configuration.

Acknowledgments

I would like to thank for the financial support of "REPUBLIC OF TURKEY PRIME MINISTRY STATE PLANNING ORGANIZATION" under grant "2002K120590/1" and Suleyman Demirel University (SDU). I also thank Dr. R. Varol and Dr. R. Kayacan for their assistance.

References

- [1] Masud J.: The Influence of Gravity on Thermocapillary Flows in High Prandtl Number Fluids. Ph.D. Thesis, Department of Mechanical & Aerospace Engineering, Case Western Reserve University, Cleveland, Ohio (1997).
- [2] Kamotani Y., Ostrach S.: Theoretical Analysis of Thermocapillary Flow in Cylindrical Columns of High Prandtl Number Fluids. Journal of Heat Transfer, 120, p. 758 (1998).
- [3] Masud J., Kamotani Y., Ostrach S.: Oscillatory Thermocapillary Flow in Cylindrical Columns on High Prandtl Number Fluids. J. Thermophysics and Heat Transfer, vol. 11, p. 105 (1997).
- [4] Chun C.-H., Wuest W.: Suppression of Temperature Oscillations on Thermal Marangoni Convection in a Floating Zone by Superimposing of Rotating Flows. Acta Astronautica, vol. 9, No. 4, p. 225 (1982).
- [5] Eckert K., Bestehorn M. and Thess A.: Square Cells in Surface-Tension-Driven Bénard Convection: Experiment and Theory. J. Fluid Mech., vol. 358, p. 149 (1998).
- [6] Boeck T. and Thess A.: Bénard-Marangoni Convection at Low-Prandtl Number. J. Fluid Mech., vol. 399, p. 251 (1999).
- [7] Chun C.-H., Wuest W.: Experiments on the Transition from the Steady to the Oscillatory Marangoni-Convection of a Floating Zone Under Reduced Gravity Effect. Acta Astronautica, vol. 6, p. 1073 (1979).
- [8] Preisser F., Schwabe D., Scharmann A.: Steady and Oscillatory Thermocapillary Convection in Liquid Columns with Free Cylindrical Surface. J. Fluid Mech., vol. 126, p. 545 (1983).
- [9] Kuhlmann, H. C., Raht, H. J.: Hydrodynamic Instabilities in Cylindrical Thermocapillary Liquid Bridges. J. Fluid Mech., vol. 247, p. 247 (1993).
- [10] Yasuhiro Kamotani, Li Wang, Sayaka Hatta, Ramazan Selver, Shinichi

Yoda.: Effect of Free Surface Heat Transfer on Onset of Oscillatory Thermocapillary Flow of High Prandtl Number Fluid. J. Jpn. Soc. Microgravity Appl., vol. 18, No. 4, pp. 283-288, (2001).

- [11] *Kamotani Y., Wang L., Hatta S., Selver R., Bhunia P. S.*: Effect of Cold Wall Temperature on Onset of Oscillatory Thermocapillary Flow. 39th AIAA Aerospace Sciences Meeting and Exhibit, Reno, NV, 8-11 January 2001.
- [12] *Ostrach S.*, in: Motion Induced by Capillarity. PhysicoChemical Hydrodynamics 2, (ed. D. B. Spalding), p. 571, Advanced Publication Co. (1977).
- [13] *Kamotani Y., Ostrach S., Vargas M.*: Oscillatory Thermocapillary Convection in a Simulated Floating-Zone Configuration. J. Crystal Growth, vol. 66, p. 83 (1984).